Int. J. Electrochem. Sci., 7 **(2012)** 12922 - 12930

International Journal of
ELECTROCHEMICAL
SCIENCE
www.electrochemsci.org

Mineralization Behavior of the Petal-Like Apatite/TiO_2 Composite Coating Prepared by Micro-Arc Oxidation

Shimin Liu[1,*], *Chunyong Liang*[2], *Hongshui Wang*[2], *Zhixia Qiao*[3]

[1] Business School, Tianjin University of Commerce, Tianjin 300134, China
[2] School of Materials Science and Engineering, Hebei University of Technology, Tianjin 300130, China
[3] School of Mechanical Engineering, Tianjin University of Commerce, Tianjin 300134, China
[*]E-mail: lshm1216@163.com

Received: 30 October 2012 / *Accepted:* 19 November 2012 / *Published:* 1 December 2012

The mineralization behavior of the petal-like apatite/TiO_2 coating, which was prepared by micro-arc oxidation (MAO) on the surface of the commercially pure titanium, was studied in simulated body fluid (SBF). The results showed that the bone-like apatite formed on the surface of the petal-like apatite layer as early as 12 h immersion in SBF. In the early immersion stage, the petal-like apatite dissolved fast into the SBF, which promoted the nucleation of the bone-like apatite, and then the nucleus of apatite grew by consuming the Ca and P ions in the SBF. It was proposed that the formation of the apatite layer on the surface of the petal-like apatite/TiO_2 composite coating in SBF followed the dissolution-precipitation mechanism.

Keywords: micro-arc oxidation; titanium; composite coating; mineralization behavior

1. INTRODUCTION

In recent years, TiO_2 coatings have attracted much attention for the excellent performance in constructing bioactive surfaces. The TiO_2 or TiO_2-based coatings that contain Ca and P can be obtained by micro-arc oxidation (MAO) in different electrolytes [1–8]. MAO is considered to be one of the most convenient and effective methods for the surface modification of titanium (Ti) and its alloys. It has been reported that porous TiO_2 coatings can effectively enhance the fixation of the implants to the bone, and at the same time improve their in vivo corrosion resistance [3, 9–11]. In order to obtain fast fixation and firm implant-bone attachment, calcium phosphate coatings are usually further prepared on the metallic implants due to the good bioactivity and osteoconductive properties [12–16]. One step synthesis of the coating consisted of HA-and TiO_2-based two layers on titanium

alloys by MAO has been reported previously [17]. The immersion behavior of TiO_2 coating, P-containing titania and anatase-based coating containing Ca and P in simulated body fluids (SBF) were studied in previous papers [2, 18, 19]. These in vitro studies are important in a practical sense in that it could give some indication of the in vivo behavior of the coating [12, 20]. However, to the best of the author's knowledge, the morphology conversion process of the calcium phosphate coating and its mineralization behavior mechanism in SBF immersion has not been investigated in detail.

In our previous studies, a petal-like apatite/TiO_2 composite coating on the surface of a commercially pure Ti was prepared by MAO [21]. The present study is to evaluate the apatite-inducing ability of the composite coating in SBF and its mineralization behavior mechanism. Based on the variations of the morphology and the Ca and P concentration in SBF immersion, the nucleation and growth of the apatite in SBF on the MAO coating was investigated in detail, which is helpful to understand the mineralization behavior mechanism in visualize.

2. EXPERIMENTAL PART

2.1. Preparation of the apatite/TiO_2 composite coating

Commercially pure Ti plates ($10\times10\times1$ mm^3) were used as the substrate for MAO treatment. Prior to MAO process, the sample surfaces were wet-ground gradually with abrasive papers to 1000#, then ultrasonically cleaned in ethanol and de-ionized water for 5 min, respectively. The MAO process was conducted with a pulsed DC power supply. The Ti plates were used as anodes while the Pt plates as cathodes in the electrolyte bath. The electrolyte was prepared by dissolving reagent-grade chemicals of $(CH_3COO)_2Ca\cdot H_2O$ (0.2mol/L) and $NaH_2PO_4\cdot 2H_2O$ (0.1mol/L) in de-ionized water. During the MAO treatment, the applied voltage, pulse frequency, duty circle and duration time were 390 V, 700 Hz, 20% and 3 min, respectively. The temperature of the electrolyte was maintained at 25 ºC by a cooling system. After the MAO treatment, the samples were cleaned with distilled water and dried in air.

2.2. SBF immersion

In order to characterize their mineralization behavior, all the samples were immersed in 1.5 SBF, in which the ion concentration is 1.5 times higher than that of the human blood plasma (as shown in Table 1). In the experiment, 1.5 SBF was used to accelerate the rate of apatite formation. The SBF was prepared by dissolving the reagent-grade mixtures of NaCl, $NaHCO_3$, KCl, $Na_2HPO_4\cdot 7H_2O$, $MgCl_2\cdot 6H_2O$, $CaCl_2\cdot 2H_2O$ and Na_2SO_4 in distilled water and buffering at pH 7.2 with 1M HCl and tris-hydroxymethyl aminomethane ($(CH_2OH)_3CNH_2$) at 37 ºC [18]. The solution was refreshed every 48 hours. After immersions for different time, i.e., 12, 24, 48, 72, 96 h, the samples were taken out from the SBF, washed by distilled water, and dried in air at room temperature.

Table 1. Ion concentrations of SBF in comparison with human blood plasma.

Ion	Ion concentration (mmol/L)		
	Blood plasma	1×SBF	1.5×SBF
Na^+	142.0	142.0	213.0
Cl^-	103.0	125.0	187.5
HCO_3^-	27.0	27.0	40.5
K^+	5.0	5.0	7.5
Mg^{2+}	1.5	1.5	2.25
Ca^{2+}	2.5	2.5	3.75
HPO_4^{2-}	1.0	1.0	1.5
SO_4^{2-}	0.5	0.5	0.75

2.3. Characterization methods

The surface morphologies of the samples were characterized by scanning electron microscopy (SEM, S-4800, Hitachi, Japan). Before the SEM examination, the surface of the samples was coated with a very thin gold film to improve its electrical conductivity. Energy dispersive X-ray spectrometer (EDS) was used to examine the elements of the apatite coating after immersion in SBF. The phase components were analyzed using X-ray diffraction (XRD, Rigaku/DMAX2500, Japan). Fourier transformation infrared spectroscopy (FT-IR) in a Nexus system was used to characterize the structure of the apatite coating after immersion in SBF. In the FT-IR experiment, the scanning resolution and range were 4 and 4000–400 cm^{-1}, respectively. After immersions of different periods of time, i.e., 0, 4, 8, 14, 20, 26, 32, 42 h, the Ca and P concentrations in the 1.5 SBF were measured by an inductively coupled plasma optical emission spectroscopy (ICP-OES, VISTA-MPX, America).

3. RESULTS AND DISCUSSION

Fig. 1(a) shows the surface morphologies of the apatite/TiO_2 coating on the surface of a MAO treated sample. The surface of the sample exhibited a petal-like microstructure. Regular assemblies of flakes in the petal-like apatite crystals can be clearly shown in the higher magnification image in Fig. 1(a). The coating consists of two different layers, with apatite as the top layer and a TiO_2 film as the inner layer (Fig. 1(b)). The average thickness of the apatite layer is about 10 μm. As for the formation mechanism of the composite coating, there are detailed descriptions in our previous study [21].

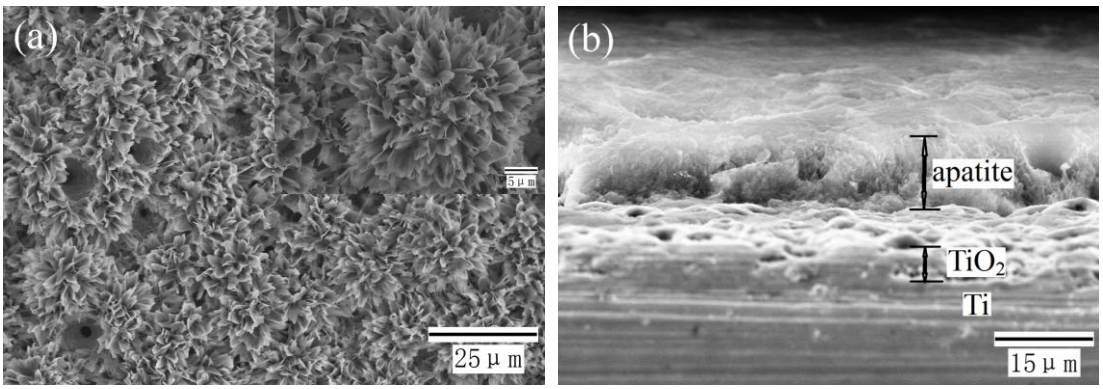

Figure 1. (a) Surface morphologies of the MAO sample, (b) cross-section view of (a)

The XRD patterns of the MAO treated sample before and after immersion in the SBF are shown in Fig. 2. The apatite/TiO_2 composite coating prepared by MAO was composed of anatase, rutile and hydroxyapatite (Fig. 2(a)). After immersion in the SBF for 96 hours, anatase and HA became the main phases (Fig. 2(b)). The stronger diffraction peaks of HA suggested the thicker HA coating after immersion in the SBF.

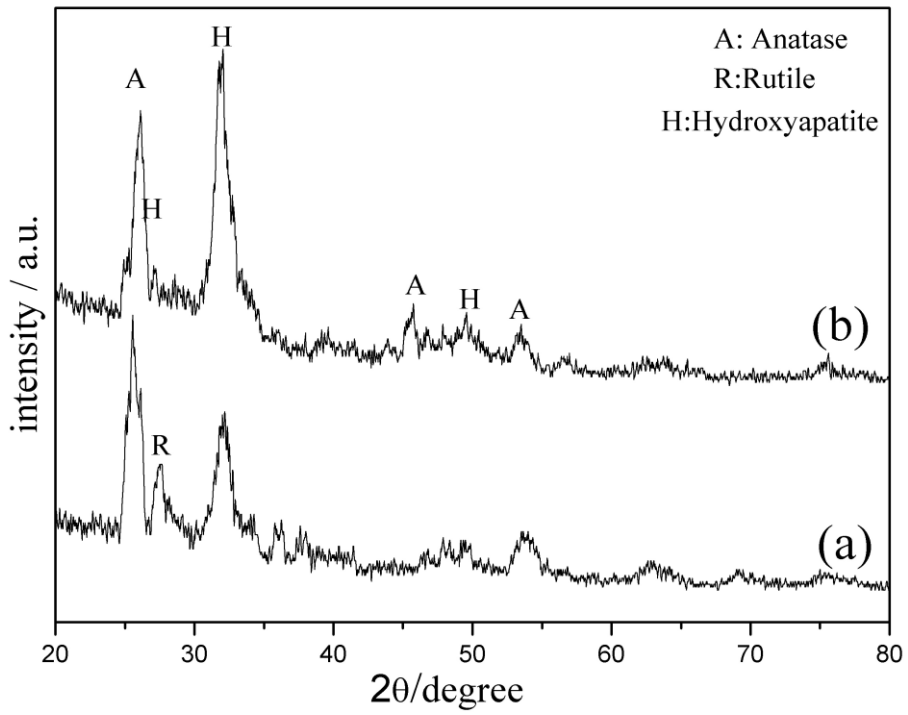

Figure 2. XRD patterns of the MAO sample (a) before and (b) after SBF immersion for 96 hours.

Fig. 3 presents the EDS profile of the sample treated by MAO after immersion in SBF for 96 hours. The elements C, O, P, and Ca were detected on the coating surface, and the Ca/P molar ratio was 1.31, indicating that the apatite layer was bone-like apatite [22].

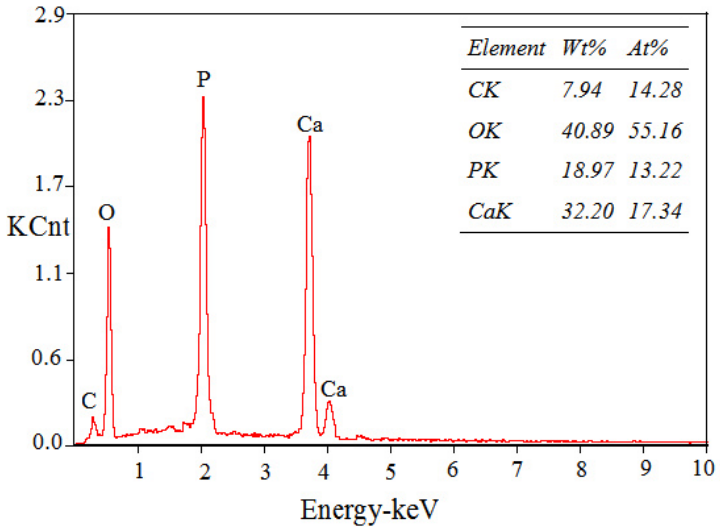

Figure 3. EDS profile of the MAO sample after immersion in SBF for 96 hours.

Fig. 4 presents the FT-IR spectra of the apatite coating scraped off from the sample after immersion for 96 hours in SBF. The spectrum shows the triply degenerated asymmetric stretching modes of ν_3PO_4 band at 1030 cm^{-1}, triply degenerated bending mode of ν_4PO_4 bands at 602 and 561 cm^{-1} [23]. The CO_3^{2-} absorption band was also detected by the characteristic stretching mode of CO_3^{2-} group at 1450 cm^{-1}, which indicates that some carbonate incorporated to the apatite and formed a carbonate-apatite similar to the human bone [24]. This was well consistent with the detection result in Fig. 3. The CO_3^{2-} in the coating after immersion came from the SBF. The broad absorption bands at 3430 and 1635 cm^{-1} in Fig. 4 were attributed to the adsorbed water [25].

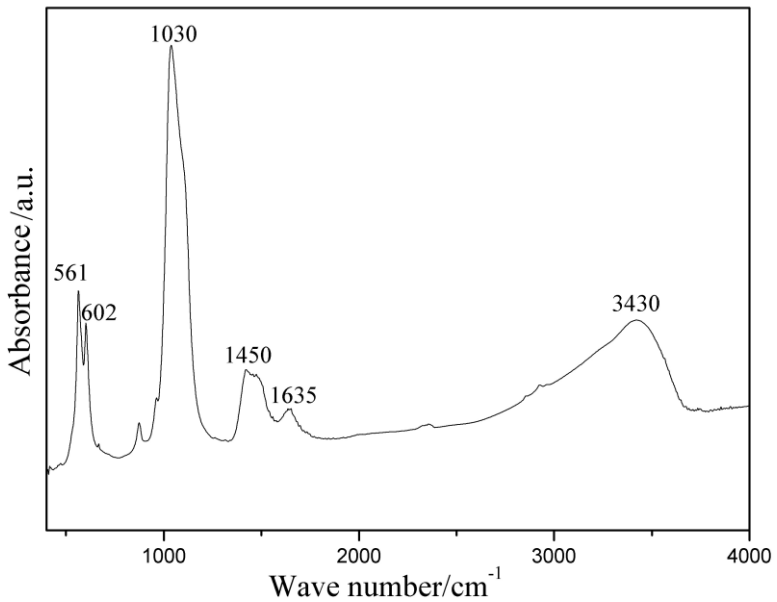

Figure 4. The FT-IR spectra of the apatite coating scraped off from the sample after immersion in SBF for 96 hours

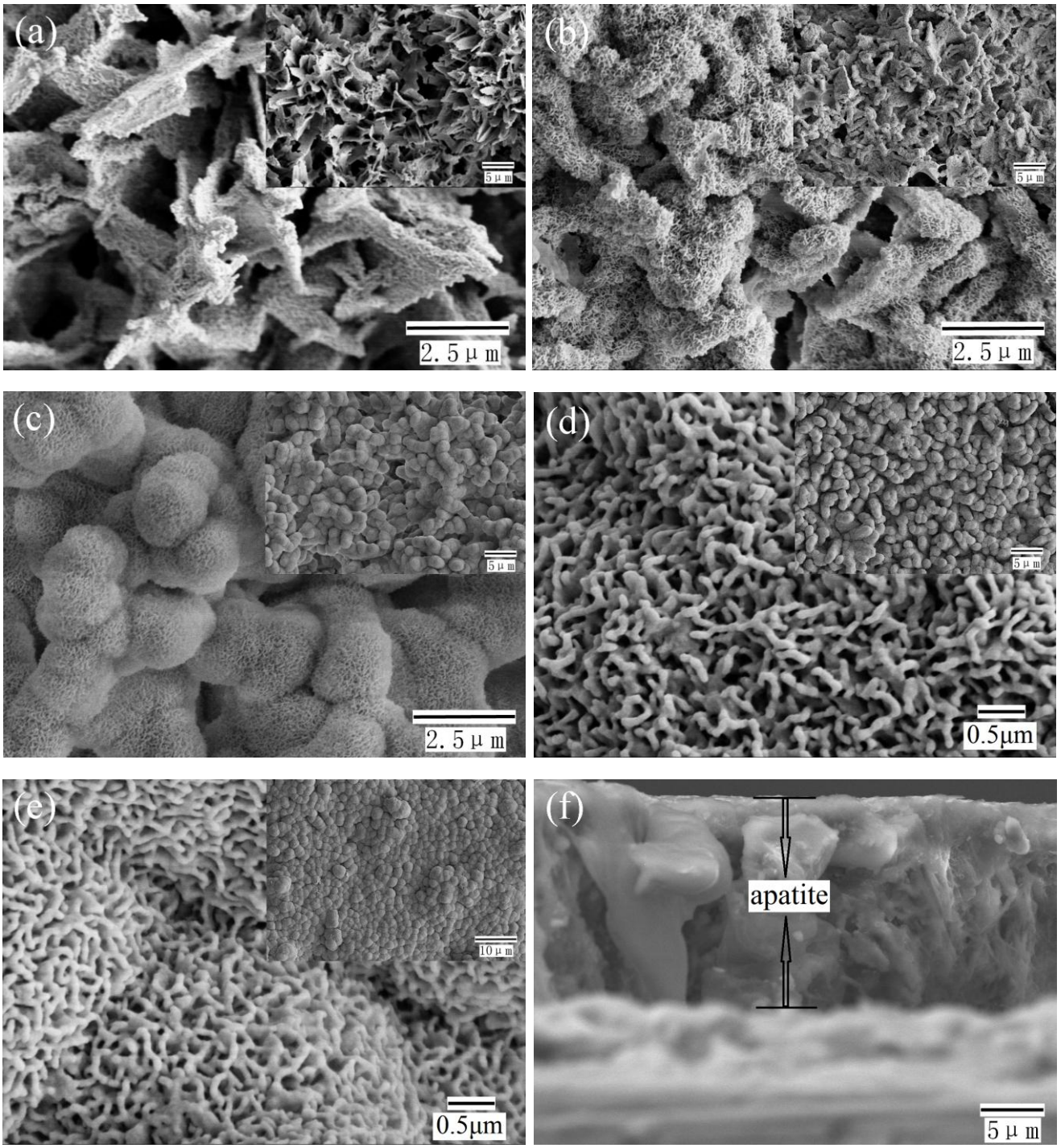

Figure 5. Surface morphologies of the samples after immersion in SBF for: (a) 12 hours, (b) 24 hours, (c) 48 hours, (d) 72 hours, (e) 96 hours, (f) cross-section view of (e).

Fig. 5 displays the surface morphologies taken from the samples after immersion in SBF for different time. After 12 hours of immersion, the petal-like structure was still obvious in the top view, but some floccules appeared on the flake surfaces (as shown in Fig. 5(a)). After 24 hours of immersion, the thickness of the flakes increased greatly and the flake edge became blunt (as shown in Fig. 5(b)). As the immersion time increased to 48 hours, most of the flakes contacted each other with

small gaps and the petal-like characteristic disappeared completely. The rod-like structure could be clearly observed in the higher magnification image (Fig. 5(c)). After 72 hours of immersion, it was found that some sphere-like particles appeared on the surface (as shown in Fig. 5(d)). With the immersion time increasing to 96 hours, the whole surface of the sample was covered with a new coating, which exhibited a network structure mainly composed of nano-scale crystals (Fig. 5(e)). Fig. 5(f) is the cross-section view of the sample in Fig. 5(e), which shows that the average thickness of the apatite layer increased to about 17 μm after 96 hours of immersion in SBF. No obvious interface was observed between the apatite coating prepared by MAO and that formed by immersion in SBF, which indicates that the two coatings can tightly adhere to each other.

Fig. 6 shows the changes of the Ca and P concentrations in the SBF as a function of the immersion time. It was noted that in the first 4 hours of immersion, there was an obvious increase both in the Ca and the P concentrations, and thereafter both of them decrease monotonously with increasing immersion time till the end of the immersion. The increases of the Ca and P concentrations at the early immersion stage indicate that the dissolution process of the apatite into the SBF occurred and was the main process. At this early stage, the higher dissolution rate led to a large number of nucleation sites on the surface of the petal-like coating. In subsequent immersion, the nucleation and growth consumed more and more Ca and P ions in the SBF and the Ca and P consumption gradually exceeded the supply from the dissolution process. Therefore the Ca and P concentrations in the SBF decreased when the immersion time exceeds 4 h [26]. This is in good agreement with the SEM micrographs shown in Fig. 5.

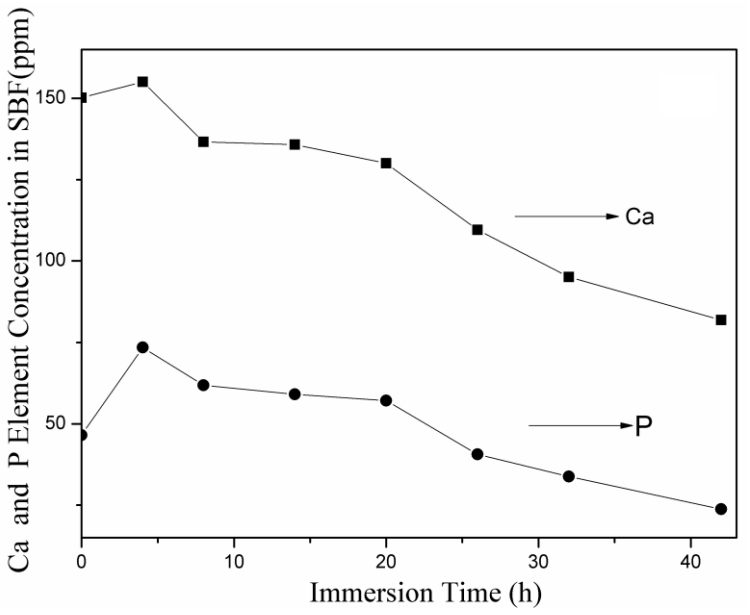

Figure 6. Ca and P concentrations of the SBF as a function of immersion time.

From the above discussion, a dissolution-precipitation mechanism is proposed to discuss the formation of the new Ca-P layer on the MAO treated surface during the immersion in SBF. The nucleation and growth of the apatite in SBF solution was a quite complex process, particularly in

physiological environments where a transient stage of intermediate phases might be involved [27]. It is well known that there are several forms of biologically relevant calcium phosphates, such as $CaHPO_4 \cdot 2H_2O$ (DCPD), $Ca_3(PO_4)_2$ (TCP), $Ca_4H(PO_4)_3$ (OCP) and HA, among which HA is the most thermodynamically stable under physiological conditions. According to the ease of nucleation and growth, the Ca-P phases rank as: DCPD > OCP > TCP > HA [28]. This order reflects the influence of the composition and crystallographic properties of calcium phosphates on their solubility. In the first stage, the least thermodynamically stable phase is the kinetically favored phase to precipitate in the SBF solution, which undergoes transformation into more stable calcium phosphates at the later stage. The precursor precipitated Ca-P phases are continuously dissolved and precipitate as hydroxyapatite by immersion in SBF for a relatively long time [29].

4. CONCLUSIONS

Petal-like apatite/TiO_2 composite coating was prepared by micro-arc oxidation at 390 V in an electrolyte containing calcium and phosphate. After immersion in SBF, a biomimetic apatite coating grew on the primary MAO coating. After immersion in SBF for 96 hours, the surface morphology of the MAO coating changed completely. The newly formed apatite was bone-like apatite. The Ca/P atom ratio was 1.31. During the early immersion in SBF, the Ca^{2+} and PO_4^{3-} in the petal-like apatite coating dissolved into the SBF and the dissolution process was the main process, and then the Ca^{2+} and PO_4^{3-} in the SBF precipitated and promoted the nucleation and growth of apatite on the surface. Dissolution-precipitation mechanism can be used to explain the formation of apatite in SBF very well.

ACKNOWLEDGEMENTS
We appreciate the National Natural Science Foundation of China (Grant No.50901029 and Grant No. 51171058) for financially supporting this work.

References

1. J.F. Sun, Y. Han and K. Cui, *Surf. Coat. Technol*, 202(2008)4248
2. D.Q. Wei, Y. Zhou, D.C. Jia and Y.M. Wang, *Ceram. Int*, 34(2008)1139
3. L.H. Li, Y.M. Kong, H.W. Kim, Y.W. Kim, H.E. Kim, S.J. Heo and J.Y. Koak, *Biomaterials*, 25(2004) 2867
4. W.H. Song, Y.K. Jun, Y. Han and S.H. Hong, *Biomaterials*, 25(2004)3341
5. M.S. Kim, J.J. Ryu and Y.M. Sung, *Electrochem. Commun*, 9(2007)1886
6. X.J. Tao, S.J. Li, C.Y. Zheng, J. Fu, Z. Guo, Y.L. Hao, R. Yang and Z.X. Guo, *Mater. Sci. Eng*. C, 29(2009)1923
7. P. Huang, K.W. Xu and Y. Han, *J. Mater. Sci. Mater. Med*, 18(2007)457
8. J.H. Ni, Y.L. Shi, F.Y. Yan, J.Z. Chen and L. Wang, *Mater. Res. Bul*, 43(2008)45
9. Y. Han, S.H. Hong and K. Xu, *Mater. Lett*, 56(2002)744
10. K.H. Park, S.J. Heo, J.Y. Koak, S.K. Kim, J.B. Lee and S.H. Kim, *J. Oral. Rehabil*, 34(2007)517
11. D.Y. Kim, M. Kim, H.E. Kim, Y.H. Koh, H.W. Kim and J.H. Jang, *Acta. Biomater*, 5(2009)2196
12. Y. Li, I.S. Lee, F.Z. Cui and S.H. Choi, *Biomaterials*, 29(2008)2025
13. C. Chen, I.S. Lee, S.M. Zhang and H.C. Yang, *Acta. Biomater*, 6(2010)2274

14. X. Bai, S. Sandukas, M.R. Appleford, J.L. Ong and A. Rabiei, *Acta. Biomater*, 5(2009)3563
15. Y. Song, S.X. Zhang, J.N. Li, C.L. Zhao and X.N. Zhang, *Acta. Biomaterialia*, 6(2010)1736
16. P. Huang, Y. Zhang, K.W. Xu and Y. Han, *J. Biomed. Mater*, 70B(2004)187
17. Y. Han, J.F. Sun and X. Huang, *Electrochem. Commun*, 10(2008)510
18. Y.W. Gu, B.Y. Tay, C.S. Lim and M.S. Yong, *Biomaterials*, 26(2005)6916
19. H.S. Ryu, W.H. Song and S.H. Hong *Surf. Coat. Technol*, 202 (2008)1853
20. M. Bohner and J. Lemaitre, *Biomaterials*, 30(2009)2175
21. S.M. Liu, X.J. Yang, Z.D. Cui and S.L. Zhu, *Mater. Lett*, 65(2011)1041
22. M.F. Chen, X.J. Yang, Y. Liu, S.L. Zhu, Z.D. Cui and H.C. Man, *Surf. Coat. Tech*, 173(2003) 229
23. S. Koutsopoulos, *J. Biomed. Mater. Res*, 62(2002)600
24. M. Lenka and A.M. Frank, *Acta. Biomater*, 2(2006)181
25. Y. Han, S.H. Hong and K.W. Xu, *Surf. Coat. Tech*, 168(2003)249
26. Y.P. Guo and Y. Zhou, *J. Biomed. Mater. Res*. A, 86(2008)510
27. Y. Leng, J.Y. Chen and S.X. Qu, *Biomaterials*, 24 (2003) 2125
28. Y.T. Xie, X.Y. Liu, P.K. Chu and C.X Ding, *Surf. Sci*, 600(2006) 651
29. M.H. Prado Da Silva, J.H.C. Lim, G.A. Soares, C.N. Elias, M.C. de Andrade, S.M. Best and I.R. Gibson, *Surf. Coat. Tech*, 137(2001)270